Published in final edited form as:
J Control Release. 2017 October 28; 264: 211–218. doi:10.1016/j.jconrel.2017.08.040.

A Non-internalizing Antibody-Drug Conjugate Based on an Anthracycline Payload Displays Potent Therapeutic Activity *in vivo*

Alberto Dal Corso[1], **Rémy Gébleux**[1], **Patrizia Murer**[1], **Alex Soltermann**[2], and **Dario Neri**[1,*]

[1)]Department of Chemistry and Applied Biosciences, Swiss Federal Institute of Technology (ETH Zürich), Vladimir-Prelog-Weg 4, CH-8093 Zürich (Switzerland) [2)]Institute of Pathology, University Hospital Zurich, Schmelzbergstrasse 12, CH-8091, Zurich (Switzerland)

Abstract

Antibody-drug conjugates are generally believed to crucially rely on internalization into cancer cells for therapeutic activity. Here, we show that a non-internalizing antibody-drug conjugate, based on the F16 antibody specific to the alternatively spliced A1 domain of tenascin-C, mediates a potent therapeutic activity when equipped with the anthracycline PNU159682. The peptide linker, connecting the F16 antibody in IgG format at a specific cysteine residue to the drug, was stable in serum but could be efficiently cleaved in the subendothelial extracellular matrix by proteases released by the dying tumor cells. The results indicate that there may be a broader potential applicability of non-internalizing antibody-drug conjugates for cancer therapy than what had previously been assumed.

Keywords

Antibodies; Protein Engineering; Vascular targeting; Antibody-Drug Conjugates; Anthracyclines

1 Introduction

The majority of small molecule anticancer therapeutics, conventionally used for cancer therapy, typically fail to localize to solid tumors.1,2 This pharmacokinetic limitation, which is becoming increasingly clear as a result of positron emission tomography studies with radiolabeled drugs in cancer patients,3 may prevent dose escalation to therapeutically active regimens and cause undesired toxicity. Antibody-drug conjugates (ADCs) have been proposed as a general approach for the generation of novel cytotoxic products, with improved therapeutic index.4,5,6,7 Two ADCs have recently gained marketing authorization: Adcetris™ for the treatment of certain hematological malignancies and Kadcyla™ for the second-line treatment of HER2-positive metastatic breast cancer.8 It is

*Corresponding Author: Tel: +41-44-6337401, neri@pharma.ethz.ch.

Disclosure of potential conflict of interest:
Dario Neri is co-founder, shareholder, and Board Member of Philogen, the company that owns the F16 antibody.

Europe PMC Funders Author Manuscripts

generally assumed that anti-cancer ADC products need to internalize into the antigen-positive tumor cells, in order to display their therapeutic action.9,10 Both antibodies and linker-payload combinations for ADC development have often been selected, on the basis of their potential to internalize into tumor cells after antigen binding and to be processed by intracellular agents.11,12 However, the strict requirement for antibody internalization has recently been questioned, as non-internalizing ADC products directed against components of the tumor extracellular matrix can efficiently liberate their drug in the extracellular space and mediate a potent therapeutic activity.13 For example, our group has shown that non-internalizing ADCs, carrying disulfide-linked drugs at site-specific positions on the antibody molecule, can release cytotoxic drugs as a consequence of tumor cell death and sub-sequent shedding of glutathione into the surrounding milieu.14,15

Until recently, studies on non-internalizing ADC products have been limited to tubulin-targeting drugs. PNU159682 has emerged as a potent anthracycline derivative, with cytotoxic activity in the picomolar concentration range.16 This compound was identified as the most active product of metabolic conversion of Nemorubicin, carried out by the CYP3A4 enzyme.17 Recently, PNU159682 was coupled to an internalizing anti-CD22 antibody: the resulting conjugate was administered to mice xenografted with cancer cell lines resistant to MMAE-bearing ADC analogues, exhibiting a significant antitumor effect. 18 In this study, we coupled a derivative of PNU159682 to the non-internalizing F16 antibody, specific to the alternatively-spliced A1 domain of tenascin-C.19 This protein is one of the most abundant markers in the stroma of solid tumors,20,21,22 lymphomas23 and in the bone marrow of acute leukemias,24 while being virtually undetectable in normal adult tissues.25,26 The resulting ADC product exhibited a potent anti-tumor effect *in vivo*.

2 Matherials and Methods

2.1 General Remarks

Experimental details on ADC characterizations and analysis of tumor sections are included in the Supporting Information file, together with an appendix with supplementary figures and mass spectra. The IgG(F16) and IgG(KSF) antibodies and the ADC product F16-MMAE were prepared as previously described.28 PNU159682 (**1**), MMAF and the linker-drug modules Mc-Val-Cit-PNU159682 (**2**) and Mc-Val-Cit-MMAF were purchased from Levena Biopharma. Fluorescein-5-Maleimide was purchased from Sigma-Aldrich.

2.2 Drug-mAb Conjugation Protocol

IgG(F16) antibody (0,9 mg/ml, 12 mg, 84 nmol) was treated with a freshly-prepared 0.1 M solution of TCEP (ACBR, 1,44 mg, 5,02 μmol, 30 eq × reactive cysteine residue) in mQ water. The mixture was reacted overnight at 4 °C. The mixture was concentrated using Vivaspin™ Turbo 15 (Sartorious) and loaded on Äkta FPLC instrument (GE Healthcare), equipped with a HiPrep 26/10 Desalting column (GE Healthcare). The reduced protein was thus purified by size exclusion chromatography, using PBS as a mobile phase, with 2 ml/min flow rate. Protein-containing fractions were pooled and concentrated in order to keep the total solution volume below the capacity limit of the FPLC-loop. The purification yielded 9 mg (70 nmol) of reduced protein, in 10 ml PBS. Compound **2** (2,2 mg, 14 μmol, 10 eq ×

reactive cysteine residue) was dissolved in DMSO (1,1 ml) and added to the reduced protein. The mixture was stirred for 1 h. at RT, the reaction was then quenched with *L*-Cysteine (Fluka) at a final concentration of 1 mM for 10 min. at RT. Final ADC F16-PNU159682 was FPLC-purified as described above, while the ADC concentration was measured following a published procedure.27 The same procedure was followed for the preparation of ADC KSF-PNU159682. ADC products were characterized by size-exclusion chromatography, SDS-Page and Mass spectrometry, as described in the Supporting Information. The ADCs were concentrated to about 1 mg/ml. Sterile-filtered aliquots were flash-frozen in liquid nitrogen and stored at -80 °C for further use. F16-MMAE and F16-MMAF ADCs were prepared and characterized following a published procedure.28

2.3 Linker stability in mouse serum

F16-PNU159682 was incubated at a concentration of 150 μg/ml in mouse serum (Invitrogen) at 37 °C in a shaking incubator. At different time points (i.e. 48, 72, 96, 120 h), aliquots were purified by affinity chromatography onto an antigen-coated resin, based on Tenascin C-A1 coupled to CNBr-activated Sepharose (GE Healthcare), washed with PBS and then eluted with 0.1 M glycine solution (pH = 3), prior to analysis by mass spectrometry. The intensity of the intact ADC signal was compared to the one of signals ascribable to PNU1596982 release from the F16 mAb (e.g. *m/z* 23373.5, relative to the mAb light chain, functionalized with the hydrolyzed Val-Cit peptide). As shown in Figure S1, no peaks ascribable to drug release were detected after 120 h.

2.4 Cell Culture

A431 epidermoid carcinoma cells (ATCC, CRL-1555) were grown in DMEM medium (Gibco) supplemented with 10% FBS (Gibco) and Antibiotic-Antimycotic (Gibco) and incubated at 37 °C in 5% CO_2 atmosphere.

2.5 Cell Viability Assays

Four human cancer cell lines (A431: epidermoid carcinoma, MDA-MB-231: metastatic breast cancer; U87: glioblastoma; SKRC-52: renal cell carcinoma) were incubated in 96-well plates for 72 h at 37 °C and 5% CO_2 with either PNU159682 (**1**) or its derivative MC-Val-Cit-PNU159682 (**2**) at different concentrations. In a second experiment, A431 cells were seeded (5000 cells/well) and incubated for 72 h with DMEM medium (Gibco, +10 % FBS) containing serial dilutions of PNU159682, MMAE and MMAF (highest concentrations tested: 5, 500 and 500 nM, respectively). The media were replaced by a solution of MTS cell viability dye (Promega) in cell medium. The plates were incubated for 3 h under culture conditions and the absorbance at 490 nm was measured on a Spectra Max Paradigm multimode plate reader (Molecular Devices). Experiments were performed in triplicate and average cell viability was calculated as measured background corrected absorbance divided by the absorbance of untreated control wells. IC_{50} values were determined by fitting data to the four-parameter logistic equation, using a Prism 6 software (GraphPad Software) for data analysis.

Europe PMC Funders Author Manuscripts

2.6 Animal Studies

Ten to twelve weeks-old female BALB/c nude mice were obtained from Janvier Laboratories (France). A431 cells (2.8×10^6 in 120 μL HBSS), were implanted subcutaneously in the flank. Tumor size was measured using a digital caliper and volume was calculated using the following formula: Tumor Size = (Length[mm]*Width^2[mm])/2. Animals were sacrificed when tumors volumes reached a maximum of 2,000 mm^3 or weight loss exceeded 15%. Experiments were performed under project licenses issued by the Veterinäramt des Kantons Zürich, Switzerland (Bew. Nr. 42/2012 and Nr. 027/15).

2.7 Therapy experiments

Sterile-filtered solutions were injected intravenously in BALB/c nude mice into the lateral tail vein, using 0.5 ml 29G insulin syringe (MicroFine™+, BD medical). Results were expressed as tumor volume in mm^3 +/- SEM. In a first therapy, mice (n = 5) were injected every 3 days, 2 times in total, with F16-PNU159682 at 2 mg/kg, or with KSF-PNU159682 at 2 mg/kg, or with vehicle (PBS). In the second therapy, mice (n = 5) were injected with F16-PNU159682, KSF-PNU159682 and vehicle (PBS) every 3 days, 2 times in total at 1 mg/kg dose, whereas F16-MMAE and F16-MMAF were administered every 3 days, 4 times in total at 7 mg/kg dose. Mice were sacrificed when tumor volume reached 2000 mm^3 or when -15% body weight loss was measured.

2.8 Flow cytometry analysis

A431 cells cultured in a T-150 flask were detached with Accutase (ThermoFisher) and stained with Fluorescein-5-Maleimide-labelled IgG(F16), IgG(KSF) and FITC-labelled anti-CD81 (BioLegend) antibodies. All staining and washing steps were performed in 2 mM EDTA 0.5% BSA in PBS. Cells were sorted by FACS (CytoFLEX, Beckman Coulter) and analyzed using FlowJo software.

2.9 Immunohistochemistry

A431 tumors excised from mice after therapy study were embedded in OCT medium (Thermo Scientific), and cryostat sections (10 μm) were cut. Tumor sections were fixed with cold acetone before blocking with 20% FCS and 2-3% BSA in PBS. Staining of the extra-domain A1 of tenascin C was performed with the following antibodies: IgG(F16) as primary antibody; rat anti-mouse CD31 (BD Biosciences) to detect endothelial cells and rabbit anti-human Fc (Bethyl) as secondary antibodies; donkey anti-rat IgG-AlexaFluor594 (Life Technologies) and goat anti-rabbit IgG-AlexaFluor488 (Life Technologies) were then used as tertiary antibodies for microscopic detection. Nuclear staining was performed with DAPI (Thermo Scientific). *Ex vivo* detection of ADCs F16-PNU159682, KSF-PNU159682 and F16-MMAF was performed using the same antibodies described above, with the exclusion of the primary antibody.

3 Results

3.1 Cytotoxic activity of ADC payload PNU159682

The cytotoxic activity of Nemorubicin metabolite PNU159682 (**1**) was compared to the one of the commercial derivative Mc-Val-Cit-PNU159682 (compound **2** in Figure 1), equipped with a maleimide functional group for coupling to cysteine residues, a Valine-Citrulline linker and a self-immolative spacer. The two compounds were subjected to *in vitro* cytotoxic assays, performed against the human cancer cell lines A431, MDA-MB-231, U87 and SKRC-52. As expected, PNU159682 displayed a potent cytotoxic activity in the subnanomolar concentration range, while compound **2** acted as a prodrug and exhibited a >100-fold reduced activity compared to the parental compound (Figure 1B).

3.2 Synthesis and characterization of ADC products

The PNU159682 derivative **2** was coupled to a recombinant version of the IgG(F16) antibody, which contains a single reactive cysteine residue at the C-terminal extremity of the light chain.28 (Figure 2). As negative control, the KSF antibody (specific to hen egg lysozyme) was used, with an identical immunoglobulin format.28 Figure 2B,C shows the analytical characterization of the resulting conjugates (termed F16-PNU159682 and KSF-PNU159682) by SDS-PAGE, size-exclusion chromatography and mass spectrometry. The resulting conjugates were obtained pure, homogeneous and they displayed the expected drug-antibody ratio (DAR) of 2. Incubation of F16-PNU159682 in mouse serum at 37 °C showed that the Val-Cit linker is stable for over 5 days under these conditions (Figure S1), in agreement with literature data.29

3.3 Therapy experiments

The therapeutic performance of the ADC products was tested in mice bearing A431 human epidermoid carcinoma xenografts. This cancer cell line exhibits a strong expression of A1 domain of tenascin-C around tumor blood vessels, as evidenced by immunohistochemical analysis (Figure 3A). Intravenous administration of the two new ADCs into tumor-bearing mice, followed by *ex vivo* immunofluorescence detection, revealed that F16-PNU159682 (but not KSF-PNU159682) efficiently localized around tumor blood vessels (Figure 3C, D).

In a first therapy experiment, we treated BALB/c nude mice with A431 tumors by administering two i.v. injections of the ADC products (2 mg/kg) or saline, starting when the neoplastic lesions had reached a size of approximately 100 mm^3. F16-PNU159682 displayed a more potent therapeutic activity, compared to KSF-PNU159682 and to the saline control group. Complete responses were observed in animals treated with the F16 derivative, and three out of five mice were cured (Figure 4A). However, substantial toxicity was revealed by body weight loss. In particular, 2 mice in the F16-PNU159682 group were sacrificed at day 27 and 1 mouse in the KSF-PNU159682 at day 23. The toxicity was due, at least in part, to tumor lysis, as a reduced body weight loss was observed in the KSF treatment group. A second therapy experiment was performed, in which two injections of ADC products at 1 mg/kg dose were administered. Although these two cycles of injections did not lead to a complete tumor eradication, mice treated with F16-PNU159682 experienced a significant stabilization (> 30 days) of the tumor volume (Figure 4B). Also in this case, control ADC

Europe PMC Funders Author Manuscripts

product KSF-PNU159682 was found to retard tumor growth, even though the tumor volumes progressively increased over the experiment. Importantly, under these experimental conditions, no acute toxicity and no significant body weight loss was observed for the groups of mice treated with the ADC products, as highlighted in Figure 4B.

3.4 Analysis of cell-killing mechanism

A microscopic hematoxylin/eosin (H&E) analysis of tumor sections, obtained three days after the second ADC injection, revealed the onset of a substantial cell death in the F16-PNU159682 treatment group, as compared to saline treatment (Figure 5). This necrosis was localized mainly in the inner part of the tumor mass, whereas vital areas were localized in the peripheral tumor regions (i.e., where nutrients are more easily provided from blood stream).

To verify that the F16-PNU159682 is generally not processed by tumor cells through receptor-mediated endocytosis, we performed flow cytometry experiments using both F16 and KSF antibodies, site-specifically labeled with Fluorescein-5-Maleimide at the engineered Cys residues. As reported in Figure 6A, the two antibodies similarly showed no binding to A431 cells, whereas the latter were strongly positive for a third fluorescent mAb, specific to the transmembrane protein CD81.30

The ability of F16-based ADCs to mediate anticancer activity *in vivo* through an extracellular payload release mechanism was also investigated by functionalizing the mAb with two closely-related dolastatin analogues (MMAE and MMAF), which strongly differ in terms of their ability to enter tumor cells. As illustrated in Figure 6B, MMAF is a hydrophilic derivative of monomethyl auristatin E (MMAE), in which the ephedrine moiety is substituted with a *C*-terminal phenylalanine residue. While MMAE and MMAF are similarly potent when released intracellularly by internalizing ADC products,31 the two drugs display very different cytotoxicity properties when added to the supernatant of tumor cell cultures. Indeed, MMAE kills various types of tumor cells in the subnanomolar concentration range, while its charged MMAF counterpart typically fails to induce cell death at concentrations below 100 nM.31 Within the ADC context, recent findings further indicate that the lipophilic MMAE payload diffuses more efficiently towards antigen-negative cells than the MMAF.32 Firstly, we incubated the A431 cancer cells with decreasing concentrations of free MMAE and MMAF payloads. In keeping with literature data, MMAE and MMAF showed IC_{50} values of 0.3 and 134 nM, respectively (Figure 6C). Subsequently, the two auristatins were coupled to the F16 antibody through a cleavable Val-Cit linker and injected four times into A431-bearing mice, at the dose of 7 mg/kg. The *in vivo* anticancer properties of the two ADCs were in line with the cytotoxic activities observed *in vitro* with the free payloads. While F16-MMAE induced a rapid tumor regression, the F16-MMAF conjugate did not display any detectable therapeutic activity (Figure 6D), in spite of its ability to efficiently localize to the tumor site, as indicated by *ex vivo* immunofluorescence analysis (Figure 6E).

Europe PMC Funders Author Manuscripts

4 Discussion

A direct internalization into the target tumor cells has often been presented as an important requirement for ADC activity. From a theoretical point of view, internalizing ADCs should be ideally suited for the delivery of cytotoxic agents into the neoplastic cells. However, most ADC products described so far rely on the use of linkers (e.g., the Val-Cit dipeptide) which are not sufficiently stable in circulation or in the tumor microenvironment. For instance, Dorywalska and co-workers have recently described carboxylesterase 1C as a potential source of proteolytic activity for the cleavage of Val-Cit linkers in the tumor extracellular milieu.33

Interestingly, recent clinical data have shown that several large B-cell lymphoma patients expressing little-to-no CD30 antigen enjoyed complete tumor remission after monotherapy with Adcetris™.34 Tumor-infiltrating immune cells (e.g. macrophages)35 may also contribute to the extracellular activation of ADC products at the tumor site.

While the ADC internalization process can be effectively monitored *in vitro*, it is extremely difficult to quantify *in vivo* (e.g., in patients) the amount of payload that is released inside the cancer cells, rather than in the extracellular environment. Our group has reported a potent anti-cancer activity for non-internalizing ADC products, which are specific to components of the modified extracellular matrix of many tumor types. Such products exhibit an efficient and selective uptake at the tumor site, as demonstrated by dosimetry studies both in mice and humans.36,37

The experimental data presented herein, indicate that non-internalizing ADC products can be potently active in preclinical models of cancer. Our findings complement previous reports on the anti-cancer activity of non-internalizing ADC products, directed against collagen IV38 and fibrin.39 It is conceivable that the Val-Cit linker, connecting the F16 antibody to PNU159682, is cleaved by proteases that are mainly intracellular (e.g., cathepsin B), but that are released in the extracellular space upon tumor cell death. The acidic tumor microenvironment may facilitate the activation of these hydrolytic enzymes, triggering drug release by proteolysis.40

We have recently shown that other peptide linkers, such as the Val-Ala peptide sequence, can be as effective as Val-Cit in releasing cytotoxic payloads in the extracellular tumor environment.41 Moreover, the data presented in this article indicate that lipophilic drugs may be the preferred type of cytotoxic payloads, as hydrophilic or charged drugs released in the extracellular environment fail to subsequently cross the tumor cell membrane. Thanks to the high potency of the anthracycline used in this study, two injections of the F16-PNU159682 conjugate (DAR = 2) at 1 mg/kg dose were sufficient to stop tumor growth for more than 20 days in all treated mice. At higher doses, tumors could be eradicated, but a substantial loss of body weight was observed. When tubulin-interacting drugs (i.e., DM1 and MMAE)14,28 were used as payloads for non-internalizing antibodies, more than three cycles of injections at > 5 mg/kg were required in order to achieve cancer cures in the same animal models. It is conceivable that tubulin poisons may preferentially kill rapidly-dividing

cells, while anthracyclines may also act against quiescent cells, both in the tumor and in normal organs, thus potentially contributing to undesired toxicity.42

5 Conclusions

Various ADC products have shown encouraging anticancer activity in preclinical cancer models, but this novel class of therapeutic agents typically fails to induce complete responses in patients with metastatic solid tumors. Alternatively-spliced isoforms of extracellular matrix proteins (e.g., fibronectin and tenascin-C isoforms) are abundant and easily accessible in perivascular areas of most solid malignancies, lymphomas and leukemias. These antigens represent promising targets for antibody-based drug delivery applications, as a selective and long-lasting antibody accumulation at the neoplastic site has been observed both in quantitative biodistribution studies in tumor-bearing mice and in imaging studies in patients with cancer.36,37,43 Payloads released in the extracellular environment may diffuse within the tumor mass, thus leading to a pharmacodynamics effect which is different from the one of internalizing ADC products. Both protease-sensitive linkers and disulfides can be conceived for drug release in the tumor extracellular space. However, it is difficult to predict clinical activity on the basis of preclinical findings, as the concentrations of extracellular proteases could be different in the two species. The findings of this study may be relevant not only for the development of non-internalizing ADC products, but also for other classes of targeted cytotoxics. For example, we and others have recently observed that small ligands directed against non-internalizing antigens (such as carbonic anhydrase IX) may be able to selectively accumulate at the tumor site44,45 and could therefore be used as antibody substitutes. Also in case of non-internalizing small molecule-drug conjugates, a potent and selective anticancer activity was observed using both disulfide46 and peptide linkers.47,48

Supplementary Material

Refer to Web version on PubMed Central for supplementary material.

Acknowledgements

Financial support from ETH Zürich, the Swiss National Science Foundation (Projects Nr. 310030B_163479/1 and SINERGIA CRSII2_160699/1), ERC Advanced Grant “Zauberkugel” (670603), Kommission für Technologie und Innovation (Grant Nr. 17072.1), Bovena Foundation and Maiores Foundation is gratefully acknowledged.

References

1). Oberoi HS, Nukolova NV, Laquer FC, Poluektova LY, Huang J, Alnouti Y, Yokohira M, Arnold LL, Kabanov AV, Cohen SM, Bronich TK. Cisplatin-loaded core cross-linked micelles: comparative pharmacokinetics, antitumor activity, and toxicity in mice. Int J Nanomedicine. 2012; 7:2557–2571. [PubMed: 22745537]

2). Cao Q, Li ZB, Chen K, Wu Z, He L, Neamati N, Chen X. Evaluation of biodistribution and anti-tumor effect of a dimeric RGD peptide-paclitaxel conjugate in mice with breast cancer. Eur J Nucl Med Mol Imaging. 2008; 35:1489–1498. [PubMed: 18373091]

3). van der Veldt AAM, Hendrikse NH, Smit EF, Mooijer MPJ, Rijnders AY, Gerritsen WR, van der Hoeven JJM, Windhorst AD, Lammertsma AA, Lubberink M. Biodistribution and radiation dosimetry of 11C-labelled docetaxel in cancer patients. Eur J Nucl Med Mol Imaging. 2010; 37:1950–1958. [PubMed: 20508935]

Europe PMC Funders Author Manuscripts

4). Alley SC, Okeley NM, Senter PD. Antibody-drug conjugates: targeted drug delivery for cancer. Curr Opin Chem Biol. 2010; 14:529–537. [PubMed: 20643572]

5). Gerber H-P, Koehnb FE, Abraham RT. The antibody-drug conjugate: an enabling modality for natural product-based cancer therapeutics. Nat Prod Rep. 2013; 30:625–639. [PubMed: 23525375]

6). Chu Y-W, Polson A. Antibody-drug conjugates for the treatment of B-cell non-Hodgkin's lymphoma and leukemia. Future Oncol. 2013; 9:355–368. [PubMed: 23469971]

7). Gébleux R, Casi G. Antibody-drug conjugates: Current status and future perspectives. Pharmacol Ther. 2016; 167:48–59. [PubMed: 27492898]

8). Chari RVJ, Miller ML, Widdison WC. Antibody-Drug Conjugates: An Emerging Concept in Cancer Therapy. Angew Chem Int Ed. 2014; 53:3796–3827.

9). Bander NH. Antibody-Drug Conjugate Target Selection: Critical Factors. Methods Mol Biol. 2013; 1045:29–40. [PubMed: 23913139]

10). Xu S. Internalization, Trafficking, Intracellular Processing and Actions of Antibody-Drug Conjugates. Pharm Res. 2015; 32:3577–3583. [PubMed: 26108878]

11). Senter PD, Sievers E. The discovery and development of brentuximab vedotin for use in relapsed Hodgkin lymphoma and systemic anaplastic large cell lymphoma. Nat Biotechnol. 2012; 30:631–637. [PubMed: 22781692]

12). Jain N, Smith SW, Ghone S, Tomczuk B. Current ADC Linker Chemistry. Pharm Res. 2015; 32:3526–3540. [PubMed: 25759187]

13). Casi G, Neri D. Noninternalizing Targeted Cytotoxics for Cancer Therapy. Mol Pharmaceutics. 2015; 12:1880–1884.

14). Perrino E, Steiner M, Krall N, Bernardes GJL, Pretto F, Casi G, Neri D. Curative properties of noninternalizing antibody-drug conjugates based on maytansinoids. Cancer Res. 2014; 74:2569–2578. [PubMed: 24520075]

15). Gébleux R, Wulhfard S, Casi G, Neri D. Antibody Format and Drug Release Rate Determine the Therapeutic Activity of Noninternalizing Antibody-Drug Conjugates. Mol Cancer Ther. 2015; 14:2606–2612. [PubMed: 26294742]

16). Quintieri L, Geroni C, Fantin M, Battaglia R, Rosato A, Speed W, Zanovello P, Floreani M. Formation and antitumor activity of PNU-159682, a major metabolite of nemorubicin in human liver microsomes. Clin Cancer Res. 2005; 11:1608–1617. [PubMed: 15746066]

17). Broggini M. Nemorubicin. Top Curr Chem. 2008; 283:191–206. [PubMed: 23605633]

18). Yu SF, Zheng B, Go M, Lau J, Spencer S, Raab H, Soriano R, Jhunjhunwala S, Cohen R, Caruso M, Polakis P, et al. A Novel Anti-CD22 Anthracycline-Based Antibody-Drug Conjugate (ADC) That Overcomes Resistance to Auristatin-Based ADCs. Clin Cancer Res. 2015; 21:3298–3306. [PubMed: 25840969]

19). Neri D, Supuran CT. Interfering with pH regulation in tumours as a therapeutic strategy. Nat Rev Drug Discov. 2011; 10:767–777. [PubMed: 21921921]

20). Borsi L, Carnemolla B, Nicolò G, Spina B, Tanara G, Zardi L. Expression of Different Tenascin Isoforms in Normal, Hyperplastic and Neoplastic Human Breast Tissues. Int J Cancer. 1992; 52:688–692. [PubMed: 1385335]

21). Dueck M, Riedl S, Hinz U, Tandara A, Möller P, Herfarth C, Faissner A. Detection of tenascin-C isoforms in colorectal mucosa, ulcerative colitis, carci-nomas and liver metastases. Int J Cancer. 1999; 82:477–483. [PubMed: 10404058]

22). Adams M, Jones JL, Walker RA, Pringle JH, Bell SC. Changes in Tenascin-C Isoform Expression in Invasive and Preinvasive Breast Disease. Cancer Res. 2002; 62:3289–3297. [PubMed: 12036947]

23). Schliemann C, Wiedmer A, Pedretti M, Szczepanowski M, Klapper W, Neri D. Three clinical-stage tumor targeting antibodies reveal differential expression of oncofetal fibronectin and tenascin-C isoforms in human lymphoma. Leuk Res. 2009; 33:1718–1722. [PubMed: 19625084]

24). Gutbrodt KL, Schliemann C, Giovannoni L, Frey K, Pabst T, Klapper W, Berdel WE, Neri D. Antibody-based delivery of interleukin-2 to neovasculature has potent activity against acute myeloid leukemia. Sci Transl Med. 2013; 5:201ra118.

25). Castellucci M, Classen-Linke I, Muhlhauser J, Kaufmann P, Zardi L, Chiquet-Eherismann R. The human placenta: a model for tenascin expression. Histochemistry. 1991; 95:449–458. [PubMed: 1714435]

26). Yamanaka M, Taga M, Minaguchi H. Immunohistological localisation of tenascin in the human endometrium. Gynecol Obstet Invest. 1996; 41:247–252. [PubMed: 8793495]

27). Gadamasetti, KG., Li, WS., Mueller, RH., Pendri, Y., Thottathil, JK. Method for preparing thioether conjugates. EP0665020A3. 1995.

28). Gébleux R, Stringhini M, Casanova R, Soltermann A, Neri D. Non-internalizing antibody-drug conjugates display potent anti-cancer activity upon proteolytic release of monomethyl auristatin E in the subendothelial extracellular matrix. Int J Cancer. 2017; 140:1670–1679. [PubMed: 27943268]

29). Doronina SO, Toki BE, Torgov MY, Mendelsohn BA, Cerveny CG, Chace DF, DeBlanc RL, Gearing RP, Bovee TD, Siegall CB, Francisco JA, et al. Development of potent monoclonal antibody auristatin conjugates for cancer therapy. Nat Biotechnol. 2003; 21:778–784. [PubMed: 12778055]

30). Vences-Catalán F, Rajapaksa R, Srivastava MK, Marabelle A, Kuo CC, Levy R, Levy S. Tetraspanin CD81 promotes tumor growth and metastasis by modulating the functions of T regulatory and myeloid-derived suppressor cells. Cancer Res. 2015; 75:4517–4526. [PubMed: 26329536]

31). Doronina SO, Mendelsohn BA, Bovee TD, Cerveny CG, Alley SC, Meyer DL, Oflazoglu E, Toki BE, Sanderson RJ, Zabinski RF, Wahl AF, et al. Enhanced activity of monomethylauristatin F through monoclonal antibody delivery: effects of linker technology on efficacy and toxicity. Bioconjugate Chem. 2006; 17:114–124.

32). Li F, Emmerton KK, Jonas M, Zhang X, Miyamoto JB, Setter JR, Nicholas ND, Okeley NM, Lyon RP, Benjamin DR, Law CL. Intracellular Released Payload Influences Potency and Bystander-Killing Effects of Antibody-Drug Conjugates in Preclinical Models. Cancer Res. 2016; 76:2710–2719. [PubMed: 26921341]

33). Dorywalska M, Dushin R, Moine L, Farias SE, Zhou D, Navaratnam T, Lui V, Hasa-Moreno A, Casas MG, Tran TT, Delaria K, et al. Molecular Basis of Valine-Citrulline-PABC Linker Instability in Site-Specific ADCs and Its Mitigation by Linker Design. Mol Cancer Ther. 2016; 15:958–970. [PubMed: 26944918]

34). Bartlett NL, Smith MR, Siddiqi T, Advani RH, O'Connor OA, Sharman JP, Feldman T, Savage KJ, Shustov AR, Diefenbach CS, Oki Y, et al. Brentuximab vedotin activity in diffuse large B-cell lymphoma with CD30 undetectable by visual assessment of conventional immunohistochemistry. Leuk Lymphoma. 2017; 58:1607–1616. [PubMed: 27868471]

35). Li F, Ulrich M, Jonas M, Stone IJ, Linares G, Zhang X, Westendorf L, Benjamin DR, Law C-L. Tumor associated macrophages can contribute to antitumor activity through FcγR-mediated processing of antibody-drug conjugates. Mol Cancer Ther. 2017; doi: 10.1158/1535-7163.MCT-17-0019

36). Aloj L, D'Ambrosio L, Aurilio M, Morisco A, Frigeri F, Caraco' C, Di Gennaro F, Capobianco G, Giovannoni L, Menssen HD, Neri D, et al. Radioimmunotherapy with Tenarad, a 131I-labelled antibody fragment targeting the extra-domain A1 of tenascin-C, in patients with refractory Hodgkin's lymphoma. Eur J Nucl Med Mol Imaging. 2014; 41:867–877. [PubMed: 24435772]

37). Heuveling DA, de Bree R, Vugts DJ, Huisman MC, Giovannoni L, Hoekstra OS, Leemans CR, Neri D, van Dongen GA. Phase 0 microdosing PET study using the human mini antibody F16SIP in head and neck cancer patients. J Nucl Med. 2013; 54:397–401. [PubMed: 23334725]

38). Yasunaga M, Manabe S, Tarin D, Matsumura Y. Cancer-stroma targeting therapy by cytotoxic immunoconjugate bound to the collagen 4 network in the tumor tissue. Bioconjugate Chem. 2011; 22:1776–1783.

39). Yasunaga M, Manabe S, Matsumura Y. New concept of cytotoxic immunoconjugate therapy targeting cancer-induced fibrin clots. Cancer Sci. 2011; 102:1396–1402. [PubMed: 21481097]

40). Choi KY, Swierczewska M, Lee S, Chen X. Protease-activated drug development. Theranostics. 2012; 2:156–178. [PubMed: 22400063]

41). Dal Corso A, Cazzamalli S, Gébleux R, Mattarella M, Neri D. Protease-Cleavable Linkers Modulate the Anticancer Activity of Non-Internalizing Antibody-Drug Conjugates. Bioconjugate Chem. 2017; 28:1826–1833.

42). Chan KS, Koh CG, Li HY. Mitosis-targeted anti-cancer therapies: where they stand. Cell Death Dis. 2012; 3:e411. [PubMed: 23076219]

43). Sauer S, Erba PA, Petrini M, Menrad A, Giovannoni L, Grana C, Hirsch B, Zardi L, Paganelli G, Mariani G, Neri D, et al. Expression of the oncofetal ED-B-containing fibronectin isoform in hematologic tumors enables ED-B-targeted 131I-L19SIP radioimmunotherapy in Hodgkin lymphoma patients. Blood. 2009; 113:2265–2274. [PubMed: 19131554]

44). Lv PC, Putt KS, Low PS. Evaluation of Nonpeptidic Ligand Conjugates for SPECT Imaging of Hypoxic and Carbonic Anhydrase IX-Expressing Cancers. Bioconjugate Chem. 2016; 27:1762–1769.

45). Krall N, Pretto F, Mattarella M, Müller C, Neri D. A 99mTc-Labeled Ligand of Carbonic Anhydrase IX Selectively Targets Renal Cell Carcinoma *In Vivo*. J Nucl Med. 2016; 57:943–949. [PubMed: 26912427]

46). Krall N, Pretto F, Decurtins W, Bernardes GJL, Supuran CT, Neri D. A Small-Molecule Drug Conjugate for the Treatment of Carbonic Anhydrase IX Expressing Tumors. Angew Chem Int Ed. 2014; 53:4231–4235.

47). Cazzamalli S, Dal Corso A, Neri D. Acetazolamide serves as selective delivery vehicle for dipeptide-linked drugs to renal cell carcinoma. Mol Cancer Ther. 2016; 15:2926–2935. [PubMed: 27609641]

48). Cazzamalli S, Dal Corso A, Neri D. Linker stability influences the anti-tumor activity of acetazolamide-drug conjugates for the therapy of renal cell carcinoma. J Control Release. 2017; 246:39–45. [PubMed: 27890855]

Europe PMC Funders Author Manuscripts

Europe PMC Funders Author Manuscripts

A

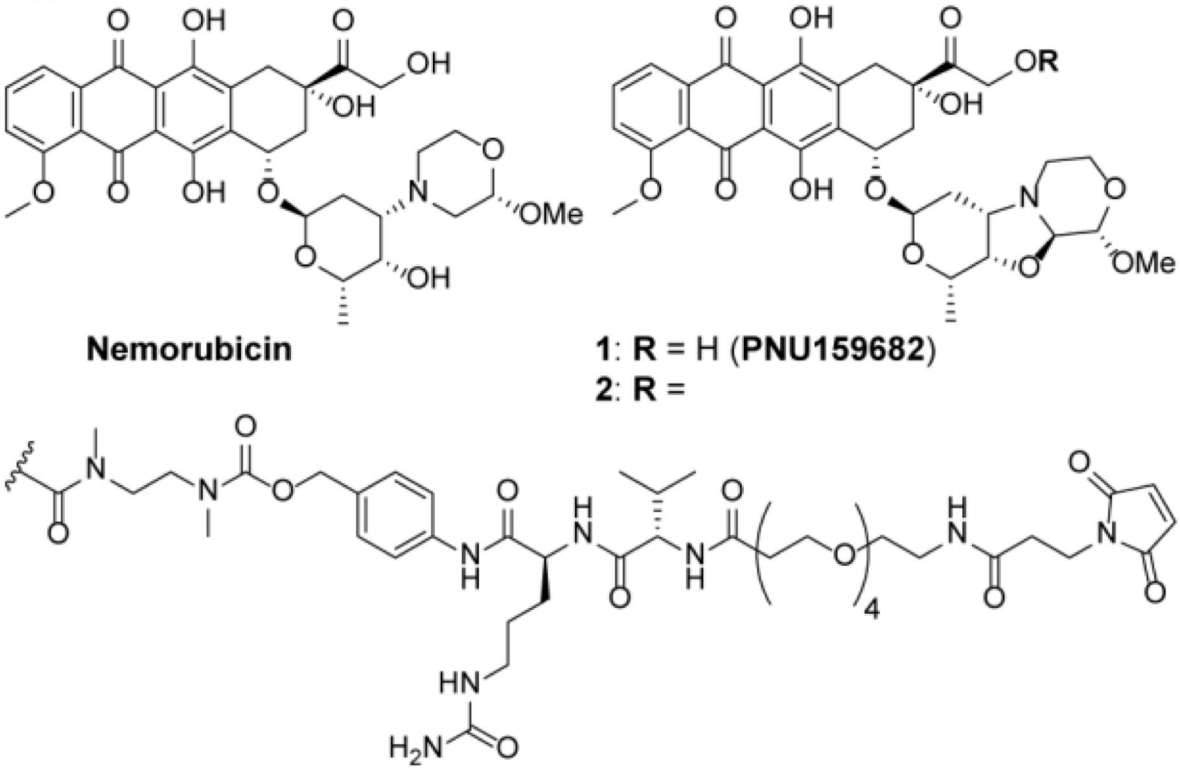

B

Cell Line	IC_{50} (nM)[a] PNU159682 (1)	Mc-Val-Cit-PNU159682 (2)
A431	0.13	23.91
MDA-MB-231	0.22	37.72
U87	0.13	13.08
SKRC-52	0.16	37.13

Figure 1.

A) Molecular structure of the anthracycline Nemorubicin, PNU159682 (**1**) and the Mc-Val-Cit-PNU159682 linker-drug module (**2**), suitable for the drug conjugation to antibodies. **B**) Antiproliferative activity of compounds **1** and **2** against four different human cancer cell lines. [a] Cytotoxic activity measured after cell incubation with 1 and 2 for 72 hours; A431: epidermoid carcinoma; MDA-MB-231: metastatic breast cancer; U87: glioblastoma; SKRC-52: renal cell carcinoma.

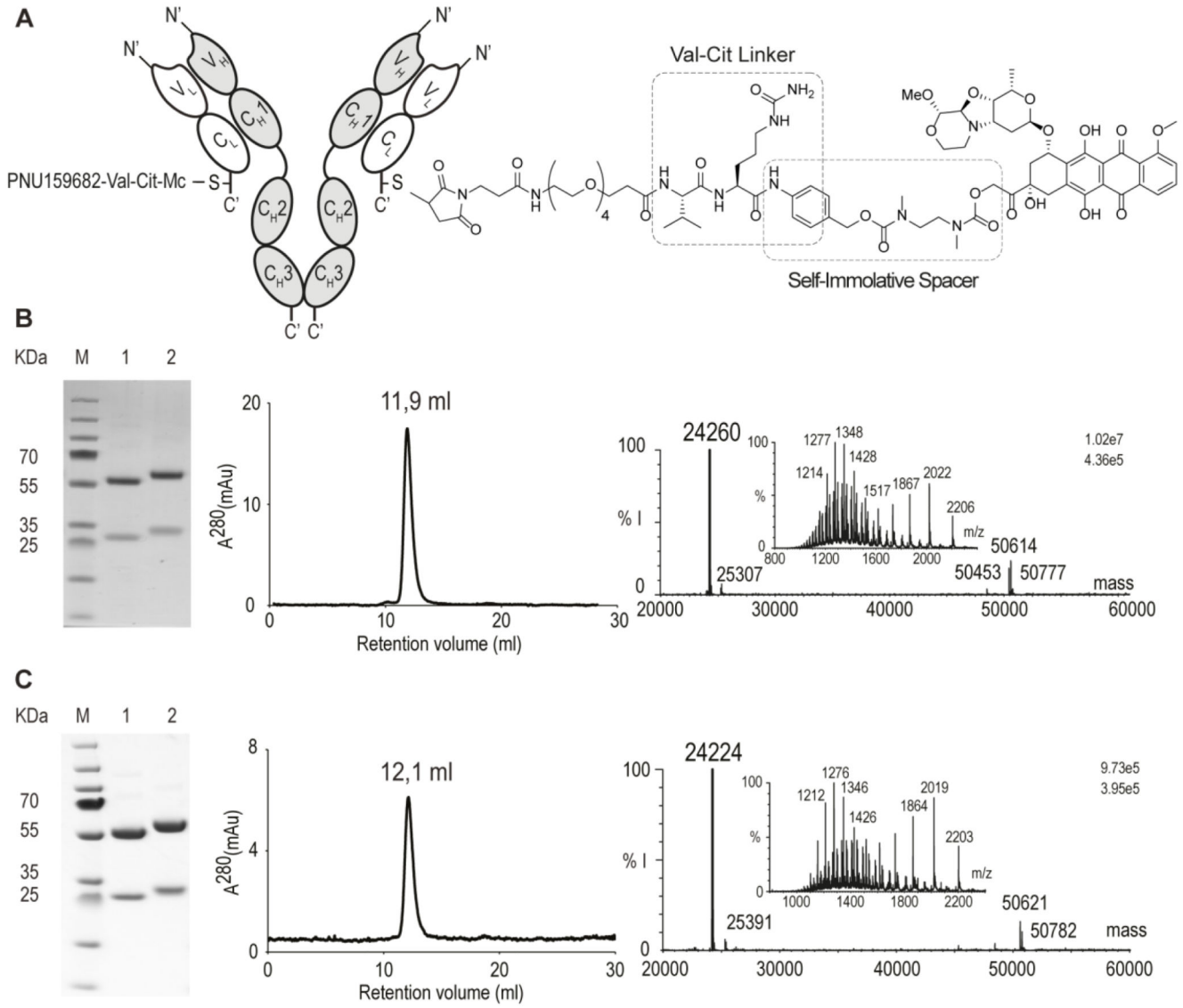

Figure 2.

Characterization of F16-PNU159682 and KSF-PNU159682. **A**) Schematic representation of the ADCs, including IgG structure and site of conjugation of the linker-drug module. **B**) SDS-page, size-exclusion chromatography profile and ESI-MS spectrum (raw and deconvoluted data) of F16-PNU159682. **C**) SDS-page, size-exclusion chromatography profile and ESI-MS spectra of KSF-PNU159682. Lanes 1 and 2 represent the final ADC in non-reducing and reducing conditions, respectively. The calculated mass of F16-PNU159682 light chain and KSF-PNU159682 light chain are 24264 (found: 24260) and 24226 Da (found: 24224), respectively (%I = % of MS intensity).

Europe PMC Funders Author Manuscripts

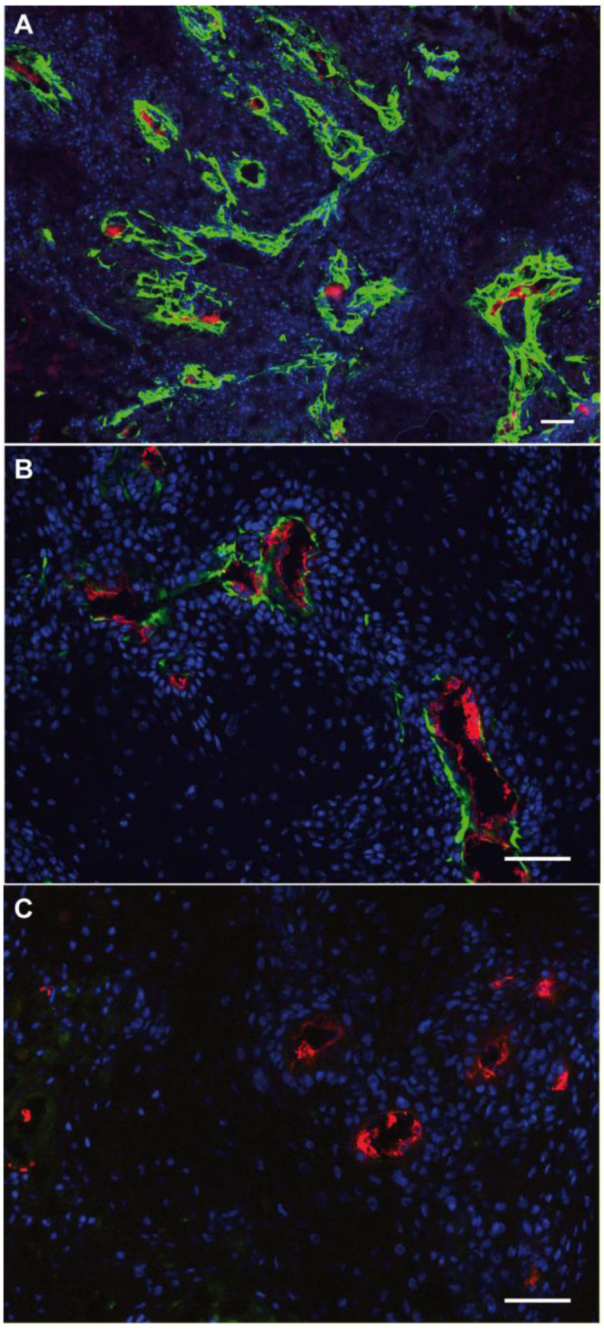

Figure 3.

A) Immunohistochemistry staining image of A431 tumor section: A1 extra-domain of Tenascin C was stained in red via biotinylated F16 antibody; *ex vivo* immunofluorescence detection of ADC compounds in A431 tumors, 48 h after i.v. injection of F16-PNU159682 (**B**) and KSF-PNU159682 (**C**). green: human IgG antibodies, red: mouse endothelial cells, blue: cell nuclei. Scale bars: 0.1 mm. While F16 was found to accumulate mainly around tumor blood vessels (3B), KSF was not detected within the experiment.

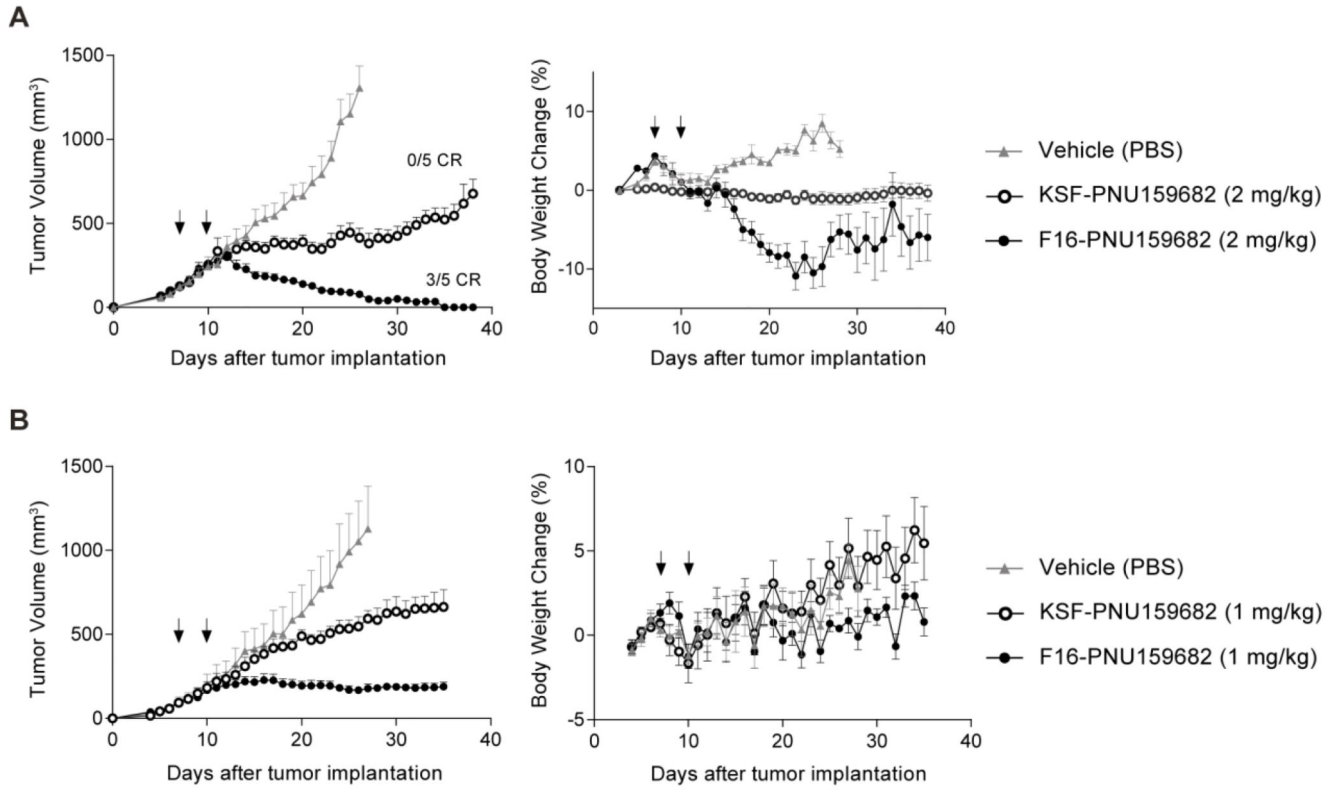

Figure 4.

Therapeutic activity of F16-PNU159682 and KSF-PNU159682 against A431 human epidermoid carcinoma xenografted in BALB/c nude mice, after 2 (B) administrations of ADCs and vehicle (PBS).in 3 days (as indicated by the arrows) at 2 (**A**) and 1 (**B**) mg/kg dose. Considering a body weight of 25 g, administration of 2 and 1 mg/kg of F16-PNU159682 and KSF-PNU159682 equals to 668 and 334 pmol of free PNU159682, respectively. Data points represent mean tumor volume ± SEM, n = 5 per group. On the right, the corresponding analysis of toxicity is reported, in terms of changes in weight of treated mice. When tumors reached 120 mm^3 volume, mice were randomly grouped (5 mice/group) and injected intravenously.

Europe PMC Funders Author Manuscripts

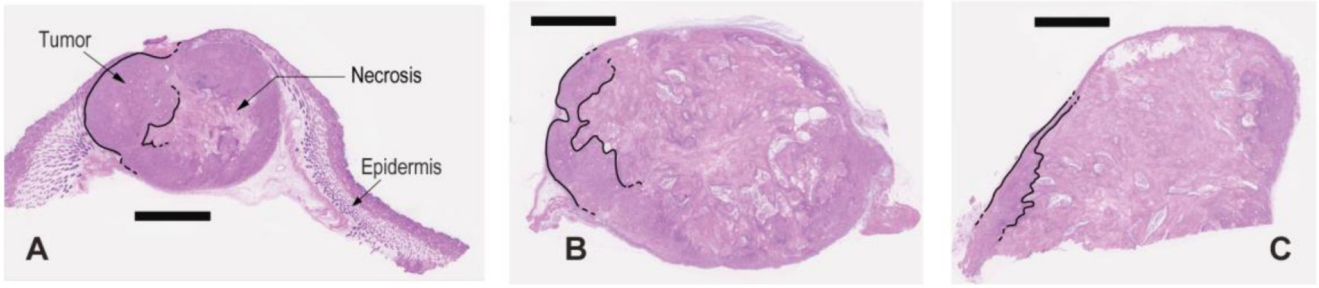

Figure 5.

H&E staining of A431 tumor sections highlighting the effects of F16-PNU159682 treatment. BALB/c nude mice were injected twice with PBS (**A**) and 2 mg/kg F16-PNU159682 (**B**, **C**), following the same schedule as for the therapy. Mice were sacrificed 3 days after their last injections (scale bar 2 mm). The cytotoxic activity displayed by F16-PNU159682 is associated to the widespread necrosis in sections images **B** and **C** (the decreasing vital mass is highlighted with black lines).

Europe PMC Funders Author Manuscripts

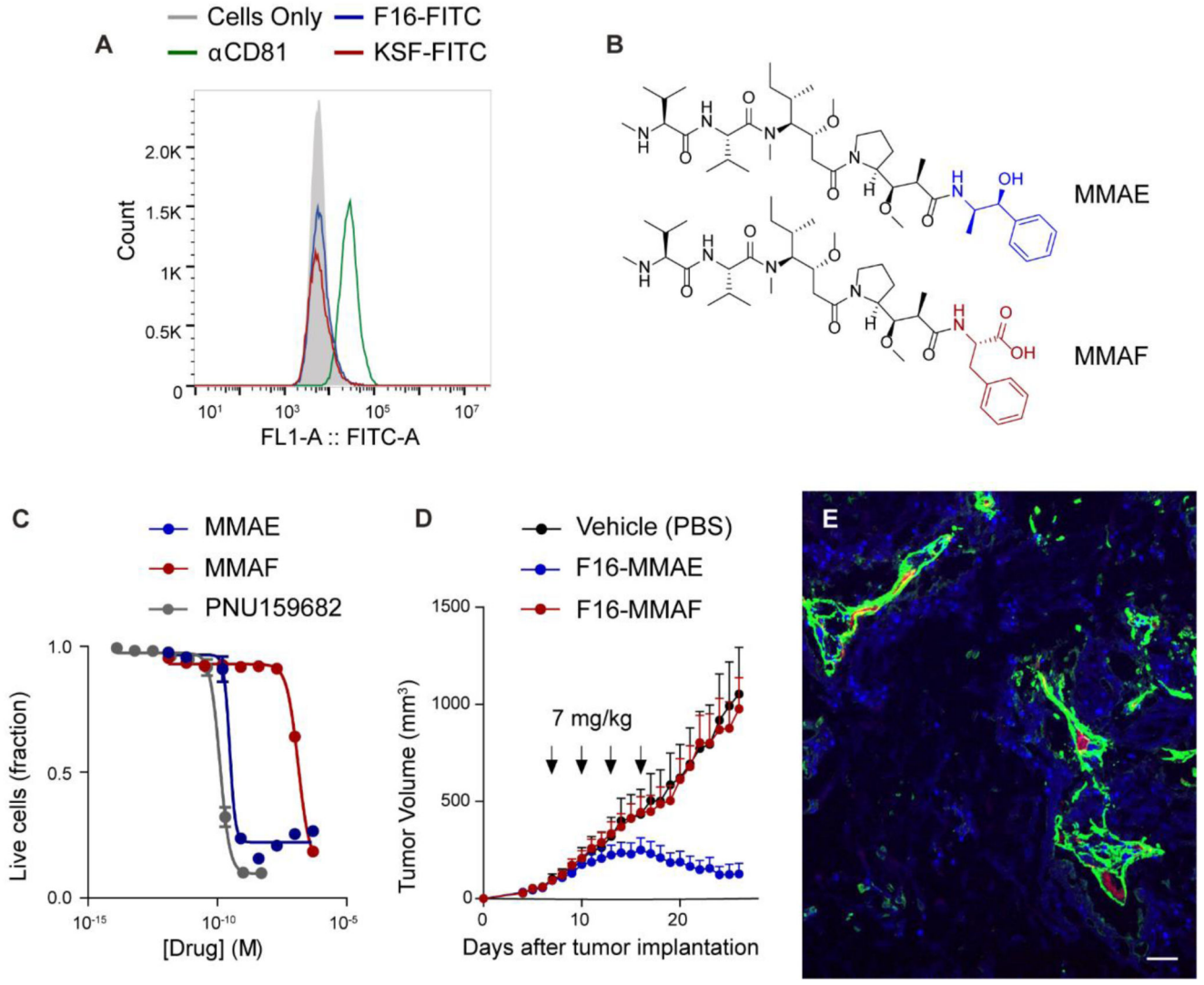

Figure 6.

A) Flow cytometry analysis of A431 cells after incubation with 3 fluorescently-labeled antibodies, specific to the A1 extra-domain of tenascin C (F16), an hen egg lysozyme (KSF) and the trasmembrane protein CD81; **B**) molecular structure of the tubulin poisons monomethyl auristatin E (MMAE) and F (MMAF); **C**) cell antiproliferative activity of free drugs PNU159682, MMAE and MMAF against A431 cancer cells; **D**) Therapeutic activity of F16-MMAE and F16-MMAF against A431 human epidermoid carcinoma xenografted in BALB/c nude mice, after 4 administrations in 12 days (as indicated by the arrows) of ADCs at 7 mg/kg dose and vehicle (PBS). Considering a body weight of 25 g, administration of 7 mg/kg of F16-MMAE and F16-MMAF equals to 2.34 nmol of free drug. Data points represent mean tumor volume ± SEM, n = 5 per group; **E**) *ex vivo* immunofluorescence detection of ADC compound in A431 tumors, 24 h after i.v. injection of F16-MMAF (green: human IgG antibody, red: mouse endothelial cells, blue: cell nuclei; scale bar: 0.1 mm).